

CHAOTIC THRESHOLD ANALYSIS OF NONLINEAR VEHICLE SUSPENSION BY USING A NUMERICAL INTEGRAL METHOD

D. ZHUANG^{1)*}, F. YU¹⁾ and Y. LIN²⁾

¹⁾State Key Laboratory of Vibration, Noise and Shock, Shanghai Jiaotong University, Shanghai 200030, China

²⁾School of Mechanical and Vehicle Engineering, Beijing Institute of Technology, Beijing 100081, China

(Received 13 December 2005; Revised 19 July 2006)

ABSTRACT—Since it is difficult to analytically express the Melnikov function when a dynamic system possesses multiple saddle fixed points with homoclinic and/or heteroclinic orbits, this paper investigates a vehicle model with nonlinear suspension spring and hysteretic damping element, which exhibits multiple heteroclinic orbits in the unperturbed system. First, an algorithm for Melnikov integrals is developed based on the Melnikov method. And then the amplitude threshold of road excitation at the onset of chaos is determined. By numerical simulation, the existence of chaos in the present system is verified via time history curves, phase portrait plots and Poincaré maps. Finally, in order to further identify the chaotic motion of the nonlinear system, the maximal Lyapunov exponent is also adopted. The results indicate that the numerical method of estimating chaotic threshold is an effective one to complicated vehicle systems.

KEY WORDS : Melnikov function, Numerical integral method, Chaotic motion, Nonlinear suspension system

1. INTRODUCTION

Since the disturbance from the road may induce uncomfortable vibration and noise in the vehicle body, it is important to study the dynamic behaviors of the vehicle. Many studies have been carried out with linear vehicle model (Ikenaga *et al.*, 2000; Hady and Crolla, 1992). However, an automobile is a nonlinear system in practice because it consists of suspension, tire and other components which have nonlinear properties. The chaotic response may appear as the vehicle moves over a rough road.

The investigation on intelligent vehicle suspension system with hysteretic damper (such as ER-fluid damper and MR-fluid damper) has been paid more and more attention in recent years (Wang *et al.*, 2003; Peel *et al.*, 1996). Hysteresis in vehicle system may lead to many complicated nonlinear dynamic behaviors, such as bifurcation and chaos. The Melnikov function is an effective analytic approach to derive the critical condition for chaotic motion of the system and has been used widely (Cveticanin, 1993; Xu *et al.*, 2005; Ge and Ku, 2000).

Based on the Melnikov function, if there is an inequality which guarantees the existence of a simple zero of Melnikov function, chaos will occur in the system. However, a number of studies on some dynamic systems

only consider the case where there exists a pair of or a single homoclinic and/or heteroclinic orbits in a non-autonomous system (Kovacic, 1993), and these analytical expressions of homoclinic and/or heteroclinic orbits can be easily obtained, so that the calculation of Melnikov functions is easy or at least is possible by using the standard integral tables or residue computations. But if a dynamic system possesses multiple saddle fixed points with homoclinic and/or heteroclinic orbits, it is impossible to obtain the analytical expressions of homoclinic and/or heteroclinic orbits in the unperturbed system. Hence, it is necessary to develop a numerical approach of Melnikov function.

The purpose of this paper is mainly to present a feasible numerical computation method to estimate the threshold of chaos and to analyze the chaotic motion of nonlinear suspension system. A vehicle model with nonlinear suspension spring and hysteretic damping element is presented as a case. The analysis of Melnikov function is performed and a criterion for the existence of chaos is derived. Based on the transformation between time variable and state variable, an algorithm for Melnikov integrals is developed for the present vehicle model. The results by analytical expression and numerical computation of Melnikov function are compared in order to verify the feasibility of the developed algorithm. At the same time, the amplitude threshold of road excitation at the onset of chaos is determined. By the numerical simulation,

*Corresponding author. e-mail: zhuangdejun@sjtu.edu.cn

the existence of chaos in vehicle system is investigated via time history curves, phase portrait plots and Poincaré maps. And the maximal Lyapunov exponent is also adopted to further identify the chaotic motion of the nonlinear system.

2. MATHEMATICAL MODEL ANALYSIS

A vehicle model with nonlinear suspension spring and hysteretic damping element is illustrated in Figure 1.

The equation of motion of vehicle system is expressed as below

$$M\ddot{z}_1 + F_s + F_d = 0 \quad (1)$$

where M is vehicle body mass, F_s is dynamic force of nonlinear suspension spring, F_d is hysteretic damping force of damper, z_1 is vertical displacement of vehicle body and z_0 is road input displacement from road excitation.

Since sinusoid forcing function can be used to describe the excitations caused by road surface roughness. Thus, the road input is approximated by the equation

$$z_0 = \eta \sin(\omega \tau) \quad (2)$$

where η and ω is amplitude and frequency of sinusoid road disturbance, respectively, and τ is time variable.

The nonlinear spring force of suspension system is assumed to have the following characteristics

$$F_s = K_s(z_1 - z_0)[1 + \alpha_s(z_1 - z_0)^2] \quad (3)$$

where K_s is equivalent stiffness and α_s is nonlinear coefficient of stiffness.

The damping force with hysteretic property is given by

$$F_d = C_d(\dot{z}_1 - \dot{z}_0)[1 + \alpha_d(\dot{z}_1 - \dot{z}_0)^2] - C_{delay}(z_1 - z_0)^3 \quad (4)$$

where C_d is damping coefficient, α_d is nonlinear coefficient of damper and C_{delay} is hysteretic coefficient. The hysteretic damping force of nonlinear suspension system

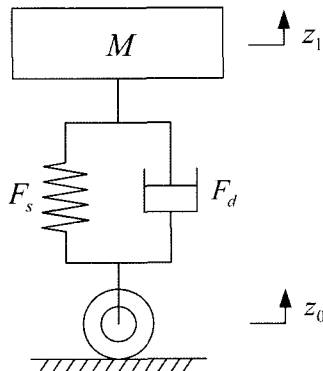


Figure 1. A vehicle model with nonlinear suspension spring and hysteretic damping element.

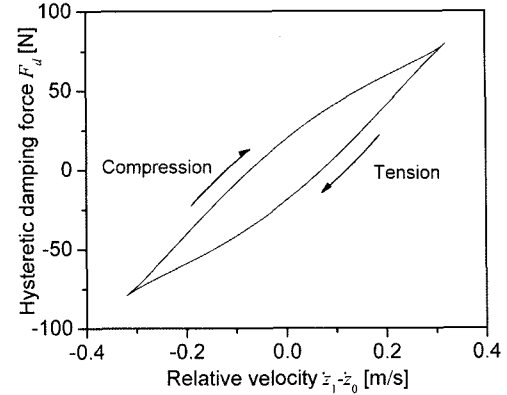


Figure 2. Hysteretic damping force of nonlinear suspension system.

is shown in Figure 2.

Defining y as the relative suspension displacement, namely, $y = z_1 - z_0$, and combining Equations (1)–(4), the equation of motion of vehicle system can be written as

$$\ddot{y} + \frac{K_s}{M}y + \frac{(\alpha_s K_s - C_{delay})}{M}y^3 + \frac{C_d}{M}\dot{y} + \frac{\alpha_d C_d}{M}\dot{y}^3 = \omega^2 \eta \sin(\omega \tau) \quad (5)$$

$$\text{Let } x = \frac{y}{\eta}, T_1 = \sqrt{\frac{M}{K_s}}, T_2 = \frac{M}{C_d}, t = \frac{\tau}{T_1}, \varepsilon = \frac{T_1}{T_2},$$

then the nondimensional equation of Equation (5) becomes

$$\ddot{x} + x + kx^3 + \varepsilon[\dot{x} + c\dot{x}^3 - f\sin(\Omega t)] = 0 \quad (6)$$

$$\text{where } k = \frac{(\alpha_s K_s - C_{delay})}{K_s} \eta^2, c = \frac{\alpha_d K_s}{M} \eta^2,$$

$$f = \frac{\omega^2 M}{C_d} \sqrt{\frac{M}{K_s}}, \Omega = \omega \sqrt{\frac{M}{K_s}}$$

Equation (6) in state space form is given by

$$\begin{cases} \dot{x}_1 = x_2 \\ \dot{x}_2 = -x_1 - kx_1^3 - \varepsilon[x_2 + cx_2^3 - f\sin(\Omega t)] \end{cases} \quad (7)$$

in which ε is small perturbation parameter. When $\varepsilon = 0$, Equation (7) becomes an unperturbed system as below

$$\begin{cases} \dot{x}_1 = x_2 \\ \dot{x}_2 = -x_1 - kx_1^3 \end{cases} \quad (8)$$

When $k > 0$, that is, $\alpha_s K_s > C_{delay}$, Equation (8) has only one fixed point $(0, 0)$; however, while $k < 0$, there exist three fixed points $(0, 0), (\pm \sqrt{-1/k}, 0)$. The eigenvalues of unperturbed system are

$$\lambda_{1,2} = \pm \sqrt{-1 - 3kx_1^2} \quad (9)$$

For the fixed point $(0,0)$, $\lambda_{1,2}=\pm i$, hence, point $(0,0)$ is a center; however, the fixed points $(\pm\sqrt{-1/k}, 0)$, $\lambda_{1,2}=\pm\sqrt{2}$, are saddle fixed points of the unperturbed system.

Since phase orbits cannot cross a center, the unperturbed system shows a stable periodic motion and the chaotic motion in the sense of Smale horseshoe cannot exist in the system when $k > 0$. Hence, the case of $k < 0$ is investigated in this paper.

When $k < 0$, Equation (8) is a planar Hamiltonian system with heteroclinic orbits. The Hamiltonian function is

$$H(x_1, x_2) = \frac{x_2^2}{2} + \frac{x_1^2}{2} + \frac{kx_1^4}{4} \quad (10)$$

As $H(\pm\sqrt{-1/k}, 0) = -1/4k$, the heteroclinic orbits of Equation (8) is shown in Figure 3.

When $\varepsilon \neq 0$ is small enough, Equation (7) may have transverse heteroclinic orbits. According to the Smale-Birkhoff homoclinic theorem (Wiggins, 1988, 1990), the existence of such orbits may result in chaotic motion.

3. MELNIKOV METHOD

The Melnikov function is an effective analytic approach to derive the critical condition for chaotic motion and has been successfully applied to some systems containing multiple saddle fixed points.

Assuming the heteroclinic orbits of Equation (8) are $q_{ij}(t) = (x_{1ij}, x_{2ij})$ and $q_{ji}(t) = (x_{1ji}, x_{2ji})$ respectively, the distances between the stable manifolds and unstable manifolds of heteroclinic orbits can be measured by Melnikov functions $M_{ij}(t_0)$ and $M_{ji}(t_0)$, in which the subscript "ij" means that the direction of the heteroclinic orbit is from x_{1i} to x_{1j} . If initial conditions for these heteroclinic orbits are properly chosen, the Melnikov functions $M_{ij}(t_0)$ and $M_{ji}(t_0)$ have simple zeros and nonzero derivatives $\dot{M}_{ij}(t_0)$ and $\dot{M}_{ji}(t_0)$, which implies the stable manifolds and unstable manifolds of heteroclinic orbits intersect transversely, that is, the chaotic

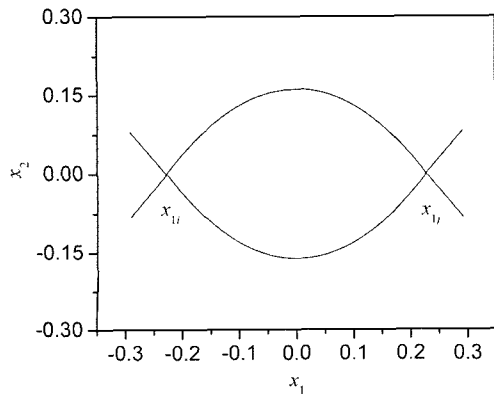


Figure 3. Heteroclinic orbits of unperturbed system.

motion may occur in the system.

The Melnikov function $M_{ij}(t_0)$ of Equation (7) for $q_{ij}(t)$ can be calculated as follows

$$\begin{aligned} M_{ij}(t_0) &= \int_{-\infty}^{\infty} x_{2ij}(t) \{-x_{2ij}(t) - c[x_{2ij}(t)]^3\} dt + \\ &\quad \int_{-\infty}^{\infty} x_{2ij}(t) f \sin(\Omega(t + t_0)) dt \\ &= -B_{ij} - cD_{ij} + f \cos(\Omega t_0) E_{ij} + f \sin(\Omega t_0) G_{ij} \\ &= -B_{ij} - cD_{ij} + f A_{ij} \sin(\Omega t_0 + \theta_{ij}) \end{aligned} \quad (11)$$

where $B_{ij} = \int_{-\infty}^{\infty} [x_{2ij}(t)]^2 dt$, $D_{ij} = \int_{-\infty}^{\infty} [x_{2ij}(t)]^4 dt$,

$$E_{ij} = \int_{-\infty}^{\infty} x_{2ij}(t) \sin(\Omega t) dt, \quad G_{ij} = \int_{-\infty}^{\infty} x_{2ij}(t) \cos(\Omega t) dt,$$

$$A_{ij} = \sqrt{E_{ij}^2 + G_{ij}^2}, \quad \theta_{ij} = \arctan(E_{ij}/G_{ij}).$$

Owing to the following symmetry equations

$$x_{1ij} = x_{1ji}(-t), \quad x_{2ij}(t) = -x_{2ji}(-t) \quad (12)$$

the Melnikov function $M_{ji}(t_0)$ for $q_{ji}(t)$ can be derived as

$$M_{ji}(t_0) = -B_{ij} - cD_{ij} - f A_{ij} \sin(\Omega t_0 + \theta_{ij}) \quad (13)$$

Based on the Melnikov method, the amplitude threshold of road excitation at the onset of chaos is obtained as

$$f|A_{ij}| \geq |B_{ij} + cD_{ij}| \quad (14)$$

Here, the equal sign corresponds to the case of tangency between the stable manifolds and unstable manifolds.

4. NUMERICAL COMPUTATION OF MELNIKOV INTEGRALS

It is important to compute the Melnikov integrals so as to verify the derived criterion. However, it is difficult to obtain the analytical expressions for some complicated dynamic systems, so numerical computations of the integrals are very necessary. Since the time variable t can be written as functions of the state variable x for heteroclinic orbits of the system (Yagasaki, 1994; Gao *et al.*, 2004), the computations of Melnikov integrals can be transformed from that for the time variable t into that for the state variable x .

Assuming $x_{1i} < x_{1j}$, according to Equation (8) and Equation (10), when $t > 0$, it yields

$$\frac{dx_1}{dt} = \mp \sqrt{2H - x_1^2 - kx_1^4/2} \quad (15)$$

By integrating Equation (15), time variable t is given by

$$t = \int_{x_{1ij}(0)}^{x_1} \frac{d\xi}{\sqrt{2H - \xi^2 - k\xi^4/2}} \quad (16)$$

According to Equation (16), the equations of B_{ij} , D_{ij} , E_{ij} , G_{ij} can be written as

$$B_{ij} = \int_{x_{1i}}^{x_{1j}} \sqrt{2H - x_1^2 - kx_1^4/2} dx_1$$

$$D_{ij} = \int_{x_{1i}}^{x_{1j}} (\sqrt{2H - x_1^2 - kx_1^4/2})^3 dx_1$$

$$E_{ij} = \int_{x_{1i}}^{x_{1j}} \sin\left(\Omega \int_{x_{1ij(0)}}^{x_1} \frac{d\xi}{\sqrt{2H - \xi^2 - k\xi^4/2}}\right) dx_1$$

$$G_{ij} = \int_{x_{1i}}^{x_{1j}} \cos\left(\Omega \int_{x_{1ij(0)}}^{x_1} \frac{d\xi}{\sqrt{2H - \xi^2 - k\xi^4/2}}\right) dx_1$$

The saddle fixed points x_{1i} and x_{1j} can be obtained by numerically solving Equation (8) and Equation (10), and the definite integrals B_{ij} , D_{ij} , E_{ij} , G_{ij} can also be numerically estimated by Simpson method.

5. COMPARISON BETWEEN NUMERICAL AND ANALYTICAL ALGORITHMS

In order to verify the validity of numerical algorithm, the analytical expression of the Melnikov function is applied as a reference in present paper. By applying the residue computations, the analytical expressions of Equation (8) are given by

$$\begin{cases} x_{1ij}(t) = \pm \sqrt{\frac{-1}{k}} \tanh\left(\frac{\sqrt{2}}{2}t\right) \\ x_{2ij}(t) = \pm \sqrt{\frac{-1}{2k}} \operatorname{sech}^2\left(\frac{\sqrt{2}}{2}t\right) \end{cases} \quad (17)$$

Substituting Equation (17) into Equation (11), the Melnikov function is computed as

$$M_{ij}(t_0) = P_{ij} \pm Q_{ij} \sin(\Omega t_0) \quad (18)$$

$$\text{where } P_{ij} = \frac{2\sqrt{2}}{3k} - \frac{8\sqrt{2}}{35k^2} C,$$

$$Q_{ij} = f\pi\Omega \sqrt{\frac{-1}{2k}} \operatorname{sech} h\left(\frac{\sqrt{2}}{4}\pi\Omega\right) \operatorname{csc} h\left(\frac{\sqrt{2}}{4}\pi\Omega\right)$$

Therefore, the condition for chaotic motion on the system satisfies

$$Q_{ij} \geq P_{ij} \quad (19)$$

In this paper, the vehicle parameters are chosen $M = 240$ kg, $K_s = 16$ kN/m, $\alpha_s = 0.5$, $C_d = 250$ N·s/m, $\alpha_d = -0.1$, $C_{delay} = 38$ kN/m by referring to Li *et al.* (2004). Based on Simpson method, the definite integrals B_{ij} , D_{ij} , E_{ij} , G_{ij} are calculated by using MATLAB in the range of the frequency $\omega \in [2, 12]$. The threshold curves of amplitude of road excitation in frequency domain are shown in Figure 4, in which the solid line is computed by the

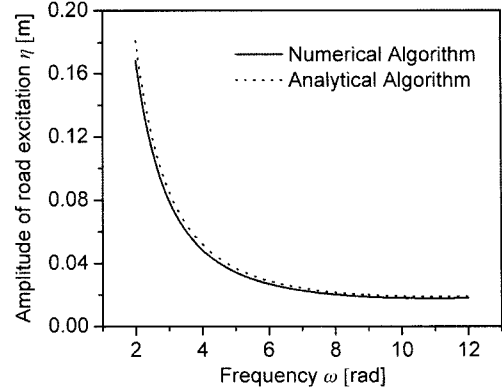


Figure 4. Threshold curves of amplitude of road excitation in frequency domain.

developed numerical algorithm; while the dotted line is computed by the analytical expression. It can be seen that the two results are in good agreement. If the amplitude η lies above the curves, the chaotic motion may occur in the present system; otherwise the motion is periodic.

6. RESULTS AND ANALYSIS

In order to express the dynamic response of the present system in detail, Equation (5) is rewritten in state space form as follows

$$\begin{cases} \dot{y}_1 = y_2 \\ \dot{y}_2 = \omega^2 \eta \sin(\omega\tau) - \frac{K_s}{M} y_1 - \frac{\alpha_s K_s - C_{delay}}{M} y_1^3 - \\ \frac{C_d}{M} y_2 - \frac{\alpha_d C_d}{M} y_2^3 \end{cases} \quad (20)$$

Equation (20) is studied numerically with the fourth order Runge-Kutta algorithm provided by MATLAB. In the computation, the fixed step size is 0.0005 and the

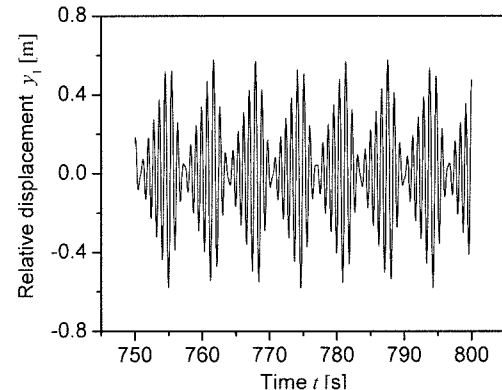


Figure 5. Time history of chaotic motion for $\eta=0.05$ m, $\omega=8$ rad.

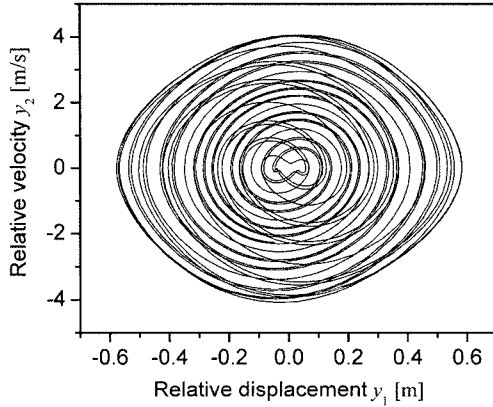


Figure 6. System phase portrait for $\eta=0.05\text{m}$, $\omega=8\text{rad}$.

absolute error tolerance is less than 10^{-6} . The initial conditions are set as $y_1=-0.01\text{m}$, $y_2=0\text{m}$. The amplitude η of road excitation is chosen as 0.05m and 0.015m when frequency of road excitation is fixed for $\omega=8$ rad by referring to Figure 4.

The dynamic responses of the present system from 0 to 800s are computed, which possess 1019 forcing cycles. To eliminate the transient responses, only the number points of last 250 periods are saved. The time history of y_1 and phase portrait of nonlinear suspension system for $\eta=0.05\text{m}$, $\omega=8$ rad are respectively plotted in Figure 5 and Figure 6.

The Poincaré map of system response is shown in Figure 7. It contains 3820 sampling points. Figure 5 through Figure 7 show that the dynamic response of nonlinear suspension system is chaotic when the amplitude and frequency of road excitation is 0.05m and 8rad, respectively.

Figure 8 through Figure 10 are respectively the time history of y_1 , phase portrait and Poincaré map of nonlinear suspension system for $\eta=0.015\text{m}$, $\omega=8\text{rad}$. It can be seen that the response of the system is a periodic motion. Chaotic motion cannot take place because the

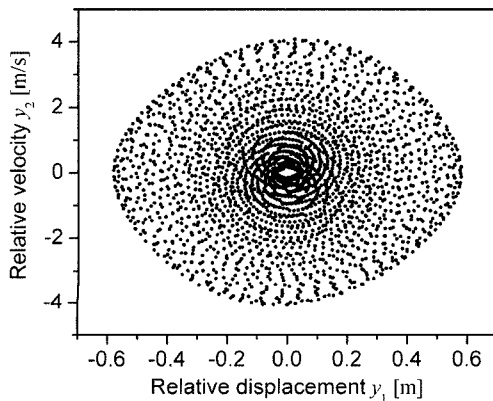


Figure 7. System Poincaré map for $\eta=0.05\text{m}$, $\omega=8\text{rad}$.

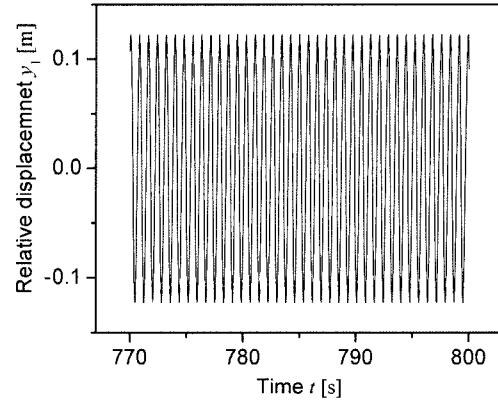


Figure 8. Time history of chaotic motion for $\eta=0.015\text{m}$, $\omega=8\text{rad}$.

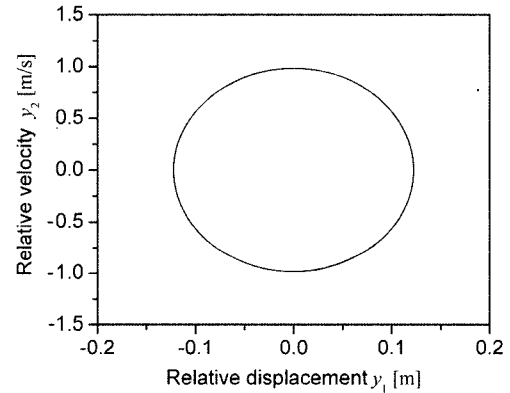


Figure 9. System phase portrait for $\eta=0.015\text{m}$, $\omega=8\text{rad}$.

amplitude of road excitation is lower than the threshold curve.

Melnikov function is a necessary condition to estimate the chaotic threshold, and can get the constant set of chaos for a nonlinear system. But it cannot judge if the system must exist a strange attractor.

If the frequency of road excitation is fixed and the amplitude of road excitation is below the threshold curve,

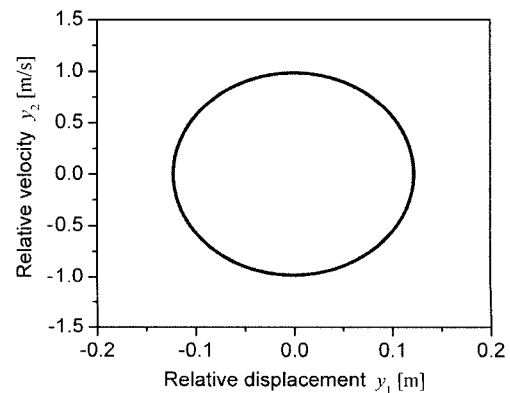


Figure 10. System Poincaré map for $\eta=0.015\text{m}$, $\omega=8\text{rad}$.

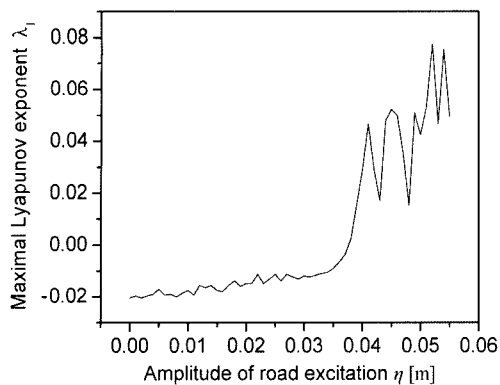


Figure 11. Maximal Lyapunov exponent for $\omega=8\text{rad}$.

the chaotic motion cannot appear in the present system. But if that is above the curve, the response of system may be transient chaos or disperse. Hence, in order to further verify the chaotic motion of nonlinear suspension system, the maximal Lyapunov exponent is also adopted in present paper.

Lyapunov exponent governs the rate of separation with respect to specific directions in phase space. Chaos is associated with a positive exponent, which implies that two orbits starting infinitesimally close to each other will diverge exponentially.

Figure 11 shows the maximal Lyapunov exponent λ_1 calculated for $\omega=8\text{rad}$ by Wolf's algorithm (Wolf *et al.*, 1985) versus the amplitude η of road excitation, in which all vehicle parameters are fixed except that η varies with increment $\Delta\eta=0.0005\text{m}$. When the amplitude of road excitation $\eta \in [0, 0.0375]$, the corresponding maximal Lyapunov exponent λ_1 is negative. It demonstrates that chaotic motion doesn't exist. When η is in the interval $[0.0375, 0.055]$, the corresponding positive maximal Lyapunov exponent indicates that the chaotic motion may occur in the nonlinear system. Because Melnikov method is a kind of theoretic approach to study chaotic motion, and it can only obtain the first order approximation of solution, the amplitude threshold of road excitation is given by the maximal Lyapunov exponent greater than that by Melnikov integrals.

7. CONCLUSION

By transforming time variable into state variable, an easy numerical algorithm of Melnikov integrals is developed for the nonlinear vehicle suspension. And the threshold curve of amplitude of road excitation is obtained in the paper. The chaotic motion may occur in the present system when the amplitude of road excitation lies above the threshold curve; otherwise the motion is periodic. And the maximal Lyapunov exponent also further verifies the conclusion. In order to eliminate the chaotic

motion in the nonlinear system, it is very necessary to develop certain control methods in the future study.

ACKNOWLEDGEMENT—This work is supported by the National Natural Science Foundation of China (50575141).

REFERENCES

- Cveticanin, L. (1993). Extension of Melnikov criterion for the differential equation with complex function. *Nonlinear Dynamics* **4**, 2, 139–152.
- Gao, H. J., Chi, X. B. and Chen, G. R. (2004). Suppressing or inducing chaos in a model of robot arms and mechanical manipulators. *J. Sound and Vibration* **271**, 3/5, 705–724.
- Ge, Z. M. and Ku, F. N. (2000). Subharmonic Melnikov functions for strongly odd non-linear oscillators with large perturbations. *J. Sound and Vibration* **236**, 3, 554–560.
- Hady, Abdel, M. B. A. and Crolla, D. A. (1992). Active suspension control algorithms for a four-wheel vehicle model. *Int. J. Vehicle Design* **13**, 2, 144–158.
- Ikenaga, S., Lewis, F. L., Campos, J. and Davis, L. (2000). Active suspension control of ground vehicle based on a full-vehicle model. *Proc. American Control Conf.* **6**, 4019–4024.
- Kovacic, G. (1993). Homoclinic and heteroclinic orbits in resonant systems. *American Society of Mechanical Engineers, Applied Mechanics Division, AMD*, **167**, 237–253.
- Li, S. H., Yang, S. P. and Guo, W. W. (2004). Investigation on chaotic motion in hysteretic non-linear suspension system with multi-frequency excitations. *Mechanics Research Communications* **31**, 2, 229–236.
- Peel, D. J., Stanway, R. and Bullough, W. A. (1996). Dynamic modelling of an ER vibration damper for vehicle suspension applications. *Smart Materials and Structures* **5**, 5, 591–606.
- Wang, E. K., Ma, X. Q., Rakheja, S. and Su, C. Y. (2003). Semi-active control of vehicle vibration with MR-dampers. *Proc. IEEE Conf. Decision and Control*, **3**, 2270–2275.
- Wiggins, S. (1988). *Global Bifurcations and Chaos*. Springer, New York.
- Wiggins, S. (1990). *Introduction to Applied Nonlinear Dynamical Systems and Chaos*. Springer, New York.
- Wolf, A., Swift, J. B., Swinney, H. L. and Vastano, J. A. (1985). Determining Lyapunov exponents from a time series. *Physica D*, **16**, 282–317.
- Xu, J. X., Rui, Y. and Zhang, W. N. (2005). An algorithm for Melnikov functions and application to a chaotic rotor. *SIAM J. Scientific Computing* **26**, 5, 1525–1546.
- Yagasaki, K. (1994). Chaos in a Pendulum with feedback control. *Nonlinear Dynamics* **6**, 2, 125–142.